Study of sea surface salinity due to river fluxes using the CMIP6 models for the Bay of Bengal region

V. Kumar, A. P. Joshi and H. V. Warrior*

Department of Ocean Engineering and Naval Architecture, Indian Institute of Technology, Kharagpur 721 302, India

The large influx of freshwater and mixing of different water masses make simulating salinity challenging for the Bay of Bengal (BoB) region. This study analyses the variability of the simulated sea surface salinity (SSS) using models present in the Coupled Modal Intercomparison Project Phase 6 (CMIP6). We collected data for 37 models from CMIP6 and validated them against the Argo (2005–14) and Aquarius (2011–14) data. Based on the skill scores, we narrowed down our search to one CMIP6 model, viz. CIESM. This model was used to study the freshwater spread (FWS) in BoB during different seasons. We found that the correlation between pH and FWS was appreciable. The CIESM model was then used to project the future trends for 10 years for the tier-1 scenario. The trend analysis of future projections revealed a positive trend in SSP1-2.6, with a decreasing trend in SSP2-4.5 and SSP5-8.5.

Keywords: Climate models, freshwater spread, river fluxes, skill score, trend analysis.

SALINITY is a key factor in the physical, chemical and biological factors of the ocean. Previous research has documented/demonstrated that the warming climate is altering the saltiness of the world's oceans, the high-salinity regions have become more saline since 1950, whereas the low-salinity regions have become more fresh. The changes in salinity patterns are likely affected by anthropogenic activities, and the large-scale effects will become more pronounced by the current 21st century[1]. The oceans hold 97% of the world's water; 80% of the rainfall received drains into the ocean; and the oceans absorb 90% of the energy released by global warming.

The Bay of Bengal (BoB) receives a large amount of freshwater from precipitation and rivers, resulting in low salinity values, especially in the northern region[2]. Surprisingly, BoB has not yet been formally/extensively studied. The variation in salinity is associated with the physical and biological properties of the waters in the region. Due to the large freshwater influx, the BoB region becomes highly stratified[3], allowing the creation of a barrier layer between the mixed and isothermal layers. Researchers have extensively examined the barrier layer in the surface-layer temperature inversion studies for this region[4,5], and it has been well simulated in the paper[6]. The formation and depth of the barrier layer for BoB are well discussed in that paper[6]. The formation of a barrier layer plays an important role in air–sea interaction processes. This layer acts as a heat barrier in the vertical heat exchanges between the mixed layer and thermocline, keeping the sea surface temperature (SST) high. The barrier layer plays a central role in keeping the BoB region less productive, by suppressing nutrients from the subsurface to the surface layers. The impact of seasonal rivers on the hydrographic characteristics of BoB has been studied[7,8]. In a modelling study[9] SSS decrease of more than 3 PSU was observed during the summer monsoon with an increase of SST by 1.5°C in the region, contributed primarily by rivers. With the inclusion of rivers, while simulating SSS in BoB, a noteworthy improvement in near-surface salinity, stratification, mixed-layer depth and barrier layer thickness was observed. This improvement in salinity-driven characteristics indicates the importance of rivers in this region.

The Coupled Model Intercomparison Project Phase 6 (CMIP6) of the World Climate Research Programme (WCRP) provides an opportunity to study several ocean general circulation models (OGCMs) simulated over the globe. The aim of this study is to provide a suite of models that can better replicate the oceans and climate. The Global Integrated Assessment Modelling (IAM) community has developed a family of different shared socio-economic pathways (SSPs) for analysing the climate change impacts of the CMIP models. CMIP6 models with natural and anthropogenic forcing provide historical simulation 1850–2014, as well as tier-1 and tier-2 future scenarios. CMIP6 tier-1 SSPs consist of SSP1-2.6, SSP2-4.5, SSP3-7.0 and SSP5-8.5 which are updated versions of CMIP5 representative concentration pathways (RCPs).

The effects of an increase in global mean temperature are already being witnessed in the melting of the Himalayan glaciers. This has increased the rate of freshwater discharge from the rivers into the oceans. The associated variations in SSS encouraged us to evaluate and analyse the simulated SSS from CMIP6 for the BoB region (6.5°–24.5°N,

*For correspondence. (e-mail: warrior@naval.iitkgp.ernet.in)

Table 1. CMIP6 SSS models (only the four best models are shown here)

Model	Centre	Experiment	Resolution (km)
CESM2-WACCM	National Center for Atmospheric Research, Community Earth System Model – Whole Atmosphere Community Climate Model, USA	Historical, SSP1-2.6, SSP2-4.5, SSP3-7.0, SSP5-8.5	100
CESM2	National Center for Atmospheric Research, Community Earth System Model – Whole Atmosphere Community Climate Model, USA		100
CESM2-WACCM-FV2	National Center for Atmospheric Research, Community Earth System Model – Whole Atmosphere Community Climate Model, USA	Historical	100
CIESM	Department of Earth System Science, China	Historical, SSP1-2.6, SSP2-4.5, SSP5-8.5	100

76.5°–100.5°E). This article evaluates the importance and applicability of studying the suitability of the CMIP6 suite of models for the hydrodynamic characteristics of BoB. Our aim was to characterize and identify the better-performing ones among the 37 CMIP6 models, which could emulate SSS for the BoB region. A comparison of each model with the satellite-derived SSS and the *in situ* salinity observations helped identify the best-performing models. These models were further explored to understand the historical trends and futuristic SSS changes for the BoB region.

Sustained interest in understanding the importance of SSS in the spread of freshwater and the pH of the waters led us to study freshwater spread (FWS) in BoB[10]. The freshwater coming from rivers spreads across the Bay in a seasonal manner, with local currents like the East Indian Coastal Current (EICC) playing a major role. In this study, we demonstrate that the influence of this FWS on the pH of the waters offers a comprehensive view of the impact of salinity on the acidification of the Bay, which in turn affects the ecosystem in the region. The ocean acidification prediction for the BoB region, as reported by Feely *et al.*[11] estimates pH to be below 8.0 by 2050 and below 7.8 in 2095. One of our major confirmations is that the ocean acidification of BoB proceeds at a lower rate than other world oceans due to FWS. These findings reinforce the general belief that salinity is a critical factor affecting sea life. BoB, being a vast reservoir of a plethora of marine life, like shells and coral reefs, the ocean acidification scenario presented by Feely *et al.*[11] concerns scientists, environmentalists and policymakers. Collectively, our findings define the importance of predicting SSS accurately throughout BoB. Further, we observed that changes in SSS had a significant impact on climate change, compared to controls, as evident from the CMIP6 models.

We have already shown in earlier works that SST plays a central/pivotal role in the flow dynamics of BoB[12,13], SST is the most widely studied feature of ocean flows and its dynamics. In this study, therefore, the intention was to introduce an additional factor, viz. SSS, also plays a pivotal role in the ocean[14] and the biological processes in BoB. In fact, central to the theory of geophysical fluid dynamics is the thermohaline flow hypothesis which states that some of the major drivers of currents in the oceans are temperature and salinity.

Data and methodology

Data

For a better understanding of climate change, CMIP6 has provided state-of-the-art OGCMs (https://esgf-node.llnl.gov/search/cmip6/). The models chosen for this study are part of the 'r1i1p1f1' ensemble. The monthly SSS data for the historical (1850–2014) and tier-1 scenarios (SSP1-2.6, SSP2-4.5, SSP3-7.0 and SSP5-8.5) were used to analyse OGCMS. The probabilistic future states (till 2100) were projected under CMIP6 tier-1 SSPs.

To analyse the variability of SSS, we have used two datasets: Argo gridded data (http://apdrc.soest.hawaii.edu/las/v6/constrain?var=204) and Aquarius OISSS gridded data (http://apdrc.soest.hawaii.edu/las/v6/constrain?var=12924). The development of Argo started in 2000; it is an international programme providing near real-time estimation of ocean state variables. These floats provide different seawater variables (e.g. salinity, temperature, chlorophyll). The Argo product has been used to improve our understanding of seawater salinity along with satellite data over the Indian Ocean. The resolution of the original Argo data is 1° × 1°. In this study, we used the monthly gridded (linearly interpolated) SSS from the Argo data, from 2005 to 2014. Aquarius satellite is a part of the Mars Pathfinder mission of NASA, USA, which provides global monthly SSS. For this study, we used the Aquarius data till 2014.

Methodology

The reference datasets and CMIP6 models have different resolutions, which were converted to the common 1° × 1° resolution (using the nearest-neighbour interpolation method) for comparison and ranking of the models. Table 1 provides a list of CMIP6 models (4 out of a total of 37) considered in this study. The monthly mean simulation output data were examined for two periods, viz. 2005–14, and 2011–14. The first simulation dataset corresponded to the Argo data (2005–14), while the other dataset corresponded to the Aquarius data (2011–14). Similar datasets have been used for validation and to calculate biases in BoB (ref. 15). Large root mean square deviation (RMSD) and negative

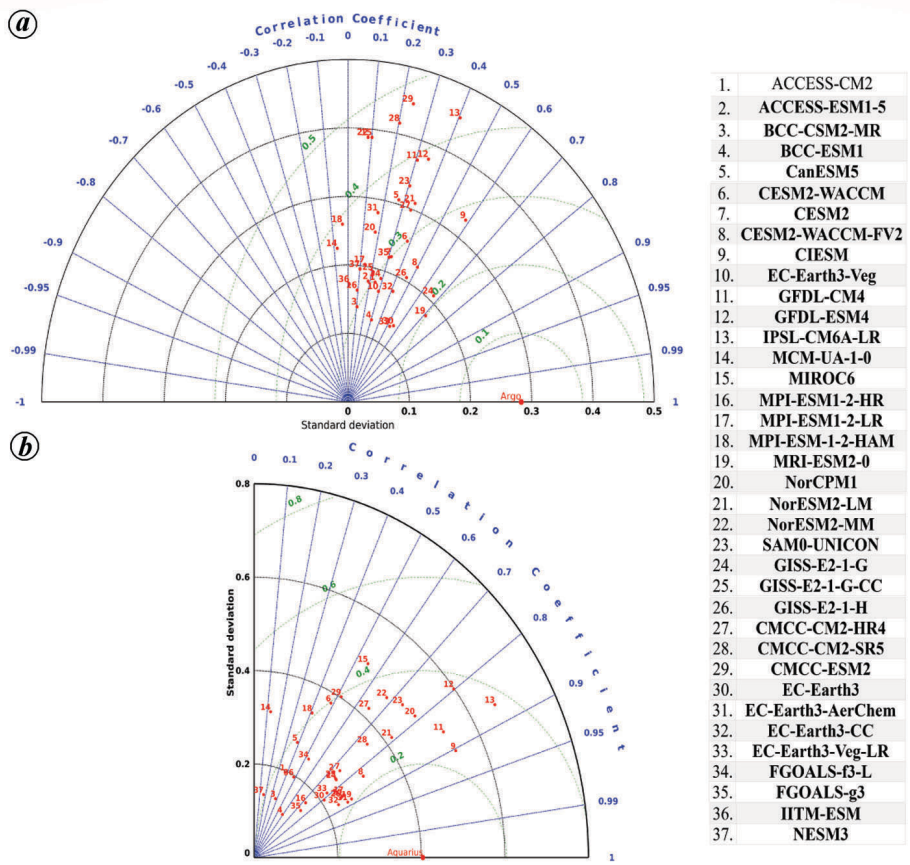

Figure 1. Taylor diagram showing the performance of the CMIP6 models with (***a***) Argo and (***b***) Aquarius data.

bias were observed along the Sumatra coast and northern BoB in the Aquarius dataset. The SSS products from the Aquarius satellite have been extensively confirmed with *in situ* observations in the Indian Ocean[16]. The Argo data SSS, evaporation (*E*) and precipitation (P) have been used to analyse ocean circulation and its impact on climate change[17].

Results and discussion

Inter-comparison of CMIP6 models with reference datasets

We made a temporal comparison between the family of CMIP6 models and the observations. We have calculated the *M*-score and Willmott skill score for all 37 models with Argo and Aquarius data. The Taylor skill score was calculated for the CMIP6 models with the observations and the Taylor diagram was drawn.

Argo data: We compared the CMIP6 models with the monthly gridded Argo data for 2005–14. Figure 1 *a* and 2 *a* show the comparison between the CMIP6 models and the Argo data using the Taylor diagram and Taylor skill score. GISS-E2-1-G (model no. 24; Figure 1) was found to be the best model, while MCM-UA-1-0 (model no. 14; Figure 1) was the worst CMIP6 model in this region. GISS-E2-1-G exhibited a correlation of 0.67, while MCM-UA-1-0 showed a negative correlation (–0.07) with the Argo data. The RMSE and standard deviation (STD) of GISS-E2-1-G were found to be 0.21 and 0.20 respectively, while MCM-UA-1-0 showed RMSE and STD values of 0.37 and 0.22 respectively. Though correlation factor (CF) and percentage bias (PB) rated both the models as 'good' (2.8 and 2.4) and 'excellent' (2.4 and 2.0), the mef for GISS-E2-1-G was in the 'good' range (0.44), but for MCM-UA-1-0 I fell in the 'poor' category (–0.73). The MCM-UA-1-0 model showed better AAE (0.69 for MCM-UA-1-0 and 0.80 for GISS-E2-1-G) and AE (0.68 for MCM-UA-1-0 and 0.80 for GISS-E2-1-G) when compared with GISS-E2-1-G. The values of absolute average error (AAE) and AE for both models were almost similar, which indicates that these models overestimate SSS in the region.

Figure 2 *b* shows the *M*-score skill of the CMIP6 models with the Argo data. This skill provided another best model (CIESM), while MCM-UA-1-0 remained the worst model. This model showed a negative *M*-score, which is rare, indicating this to be one of the least suitable models for simulating SSS. The CIESM model showed a correlation of 0.58 with the Argo data and RMSE of 0.28. The CIESM

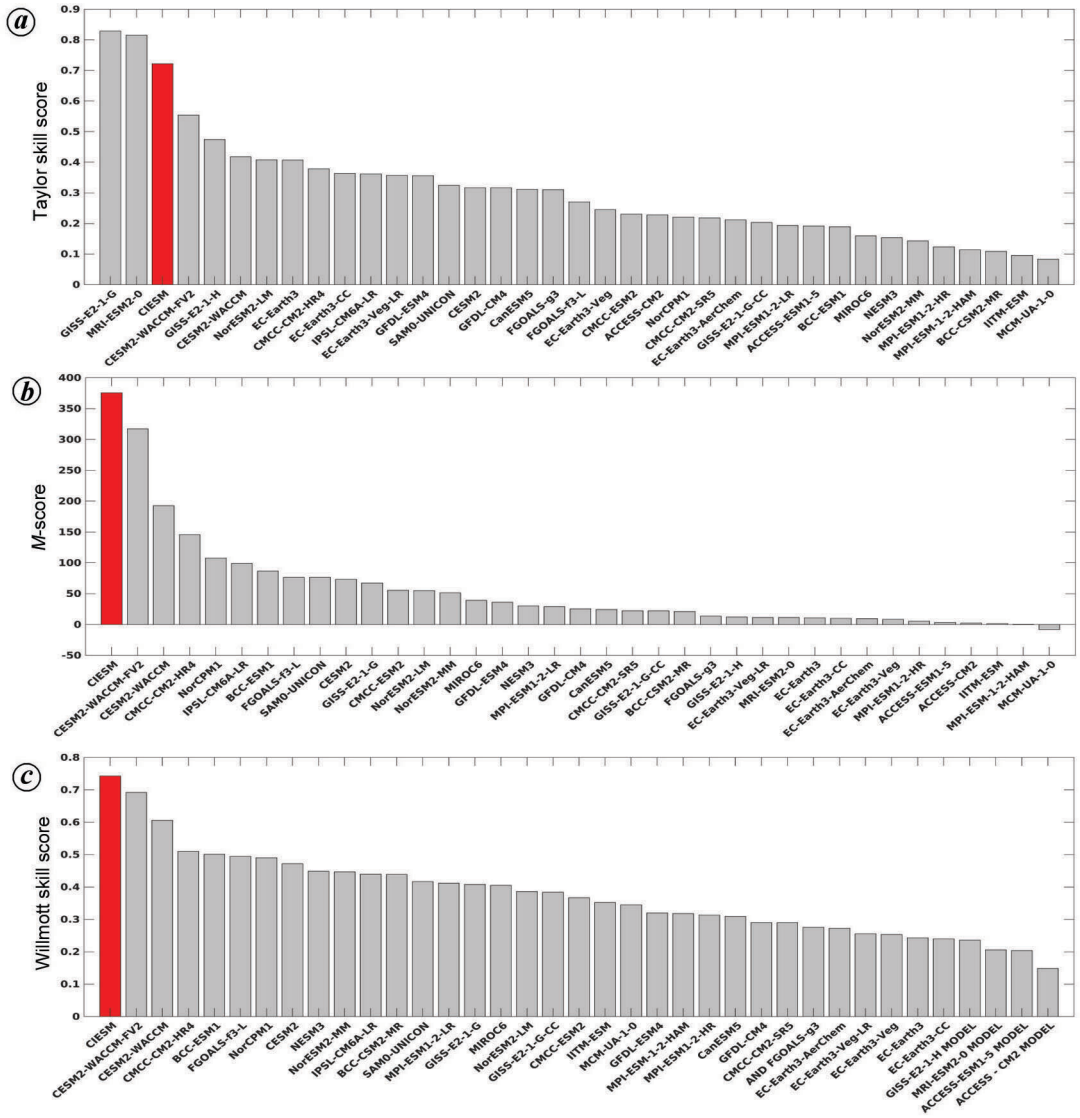

Figure 2. Skill score bar plots of CMIP6 models for three skills with Argo data: (***a***) Taylor skill score, (***b***) *M*-score and (***c***) Willmott skill score.

model showed CF (0.81) and PB (0.27) values in the 'excellent' range. AAE and AE for the CIESM model were 0.23 and 0.09, but mef was poor.

In the case of Willmott skill score, the best model was CIESM and the worst was ACCESS-CM2 (Figure 2 *c*). ACCESS-CM2 was poorly correlated (0.24) and had an RMSE of 0.29. The mef value for the model was found to be negative (–0.1). The model has an STD of 0.18; CF (10.01) rated the model as 'poor', but PB was in the 'excellent' range (8.56). Both AAE and AE were 2.82 for the ACCESS-CM2 model.

Aquarius data: Next, we compared the CMIP6 models with the Aquarius data for 2011–14. From the Taylor diagram (Figure 1 *b*) and the Taylor skill score (Figure 3 *a*), we observed that CIESM (model no. 9; Figure 1) performed the best, while NESM3 (model no. 37; Figure 1) was the worst performing model. The CIESM model showed a good correlation (0.90), while NESM3 was poorly correlated (0.15). RMSE of the CIESM model was 0.24, and the model has an STD of 0.13. CF (0.48) and PB (0.01) rated the CIESM model to be 'excellent', while mef (0.64) ranked it as 'very good'. Although CF (1.18) and PB (1.23) rated the NESM3 model as 'good' and 'excellent', mef (–0.01) showed the model to be poor. The CIESM model showed AAE of 0.19 and AE of 0.002, while the NESM3 model showed AAE and AE as 0.46 and 0.40 respectively.

We obtained the same best (CIESM) and worst (ACCESS-CM2) models in the case of *M*-score and Willmott skill score. CIESM was the best-rated model according to all three skill scores. The ACCESS-CM2 model showed a correlation of 0.37, RMSE of 0.37, and STD of 0.20. CF and mef rated the ACCESS-CM2 model as 'poor', while PB placed it in the 'excellent' category. The AAE and AE

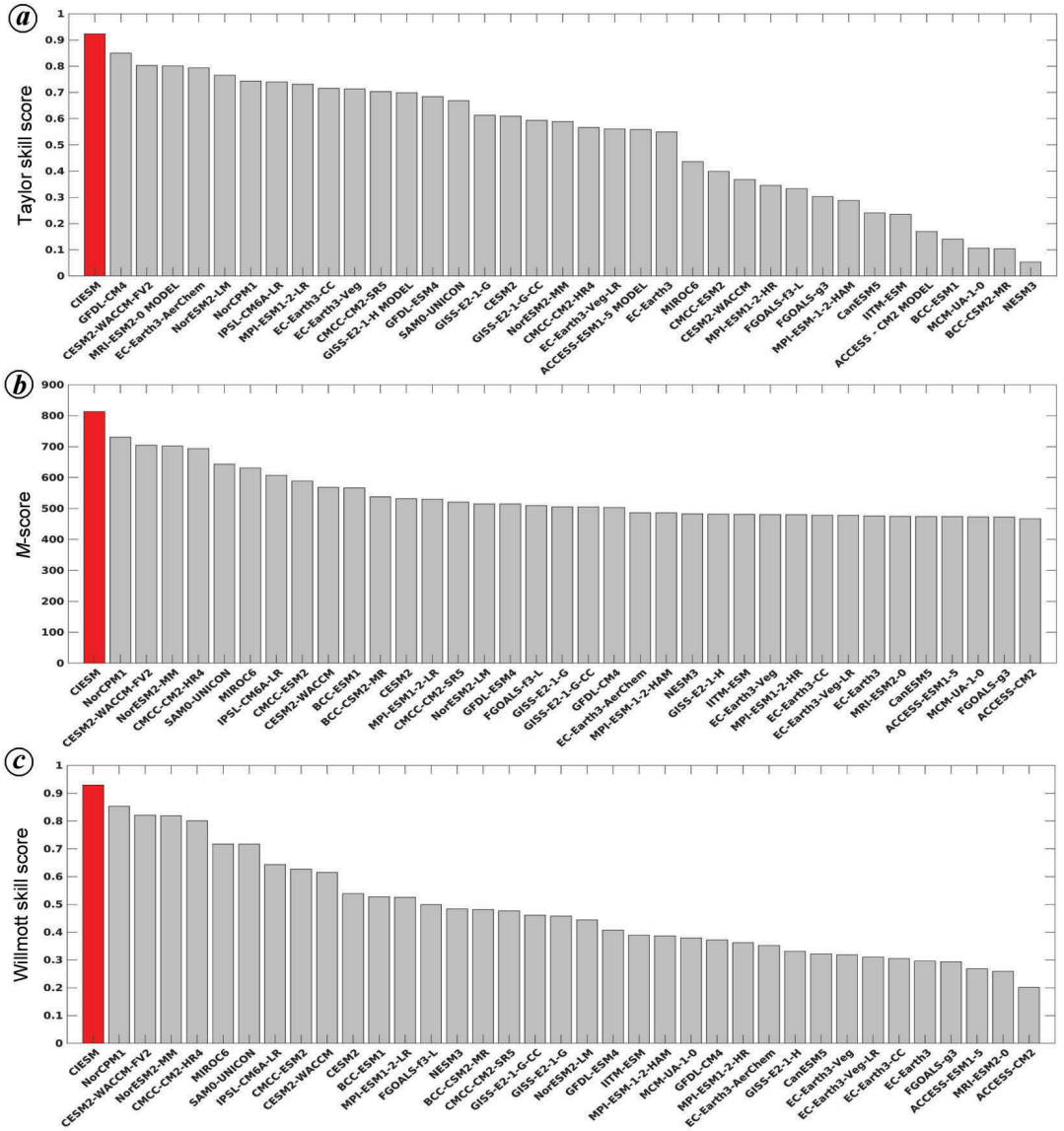

Figure 3. Skill score bar plots of CMIP6 models for three skills with Aquarius data: (***a***) Taylor skill score, (***b***) *M*-score and (***c***) Willmott skill score.

values for this model were 2.91, which is high, as seen previously with the Argo data.

We chose the best model (CIESM; marked in red in Figures 2 and 3), which features at the top according to the highest skill scores (from the Argo and Aquarius data). The CIESM model was then used for spatial and future projections.

Fresh plume spread

One of the key purposes of studying the salinity spread in the seas is to forecast and explain the development of freshwater plumes. In this section, we try to introduce this feature and compare the difference between the CIESM model (as measured against the Aquarius dataset) to predict the spread of freshwater plumes from rivers into BoB.

Figure 4 shows the SSS distribution before and after the summer monsoon, which was modelled using CIESM. It can be seen that the freshwater plume originating in the rivers penetrates deep into the bay mostly after the southwest monsoon (SWM) rainfall (by August). The figure reveals that in the northern bay, these are the waters that are brought in by the rivers during the SWM season (June–August) and collected there. Post-monsoon, it penetrates southwards (Figure 4).

The subplots in Figure 4 reveal freshwater spreading south, from August through December, when salinity decreases to 31 psu (Figure 4 *a*, *b*, northeast winter). By this period, the northward flow becomes evident; it begins to move to the right at 21°N. As a result, the northward flow along the west Odisha/Bengal coast becomes less intense. At a depth of around 150 m, salinity of the water drops

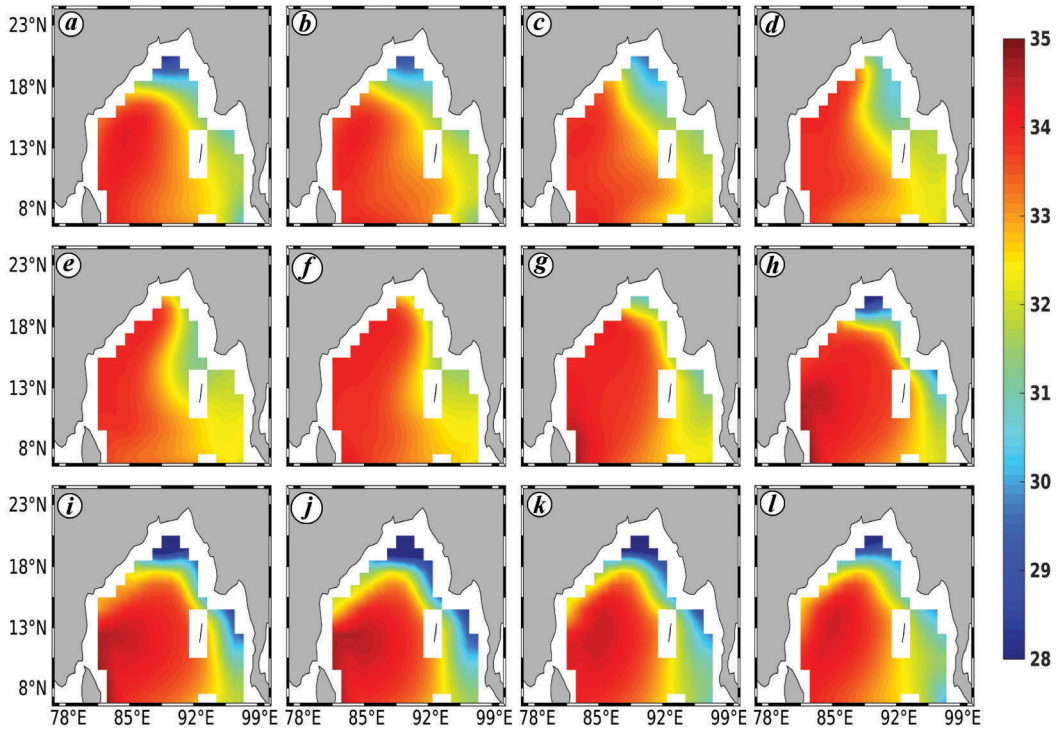

Figure 4. Salinity contours from CIESM model for 12 months of a year.

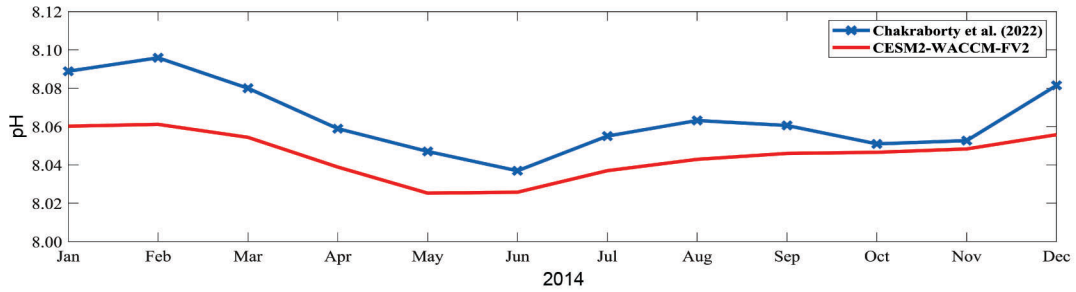

Figure 5. Comparison of pH for 2014 between CESM2-WACCM-FV2 and a study by Chakraborty *et al.*[20].

even lower, as seen from Argo profiles, from 31 psu to 30 psu (Argo data).

When comparing October and September, SSS in southern Bay is significantly low. The MODIS images (not shown here), show that there is high chlorophyll content (about 0.6 mg/l) along the coastal Bay between June and August, due to upwelling. During August to December, the waters are less saline and highly stratified, leading to less upwelling and hence no productivity. This is an interesting finding, and it could be hypothesized that freshwater and thus SSS are important triggers to prevent upwelling and for primary productivity.

SSS is lower in October than in August, with salinity reaching 30 psu across a vast section of the ocean's surface in some areas (Figure 4 *j*, October). SWM has fully dissipated and the flow in this region is now predominantly southwards. Winter sets in and SSS begins to increase due to deep convection. These results demonstrate the adequacy of CIESM in predicting the future of FWS in BoB.

pH distribution

Here we discuss the effect of SSS on pH. This is inspired by the work of Sreeush *et al.*[18], in which SST and dissolved inorganic carbon (DIC) were identified as the main drivers of the seasonality of pH in the western Arabian Sea. Sridevi and Sarma[19], observed warming and a drop in salinity, which were both associated with an increase in pH in the eastern and southern bays throughout the year. Their study[19] reveals that surface ocean pH and pCO_2 in BOB are primarily controlled by the increase in freshwater input and deposition of air pollutants in the last two decades[20].

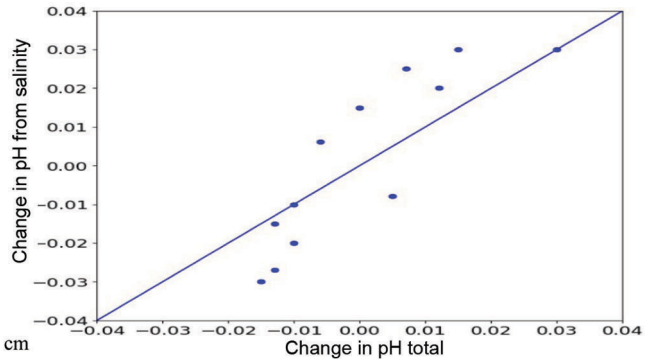

Figure 6. Correlation between pH and sea surface salinity (SSS) for CESM-WACCM-FV; $R^2 = 0.87$.

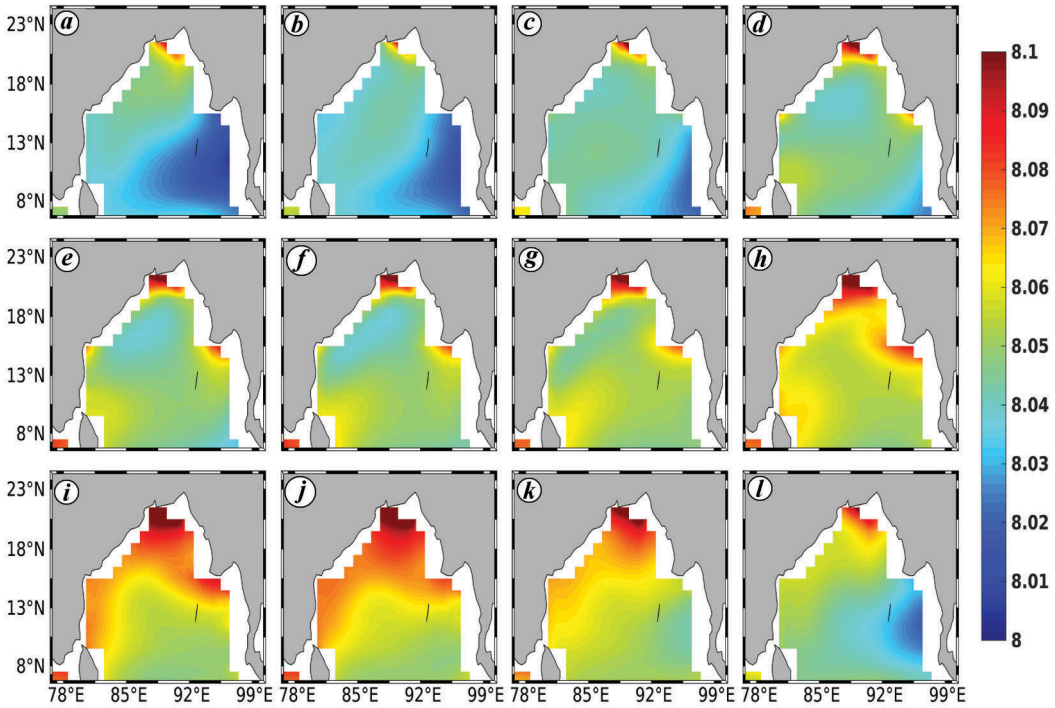

Figure 7. pH contours for the second best model, viz. CESM-WACCM-FV.

Seasonal pH variation for 2014 was compared with a recent study[21] for 2014 (Figure 5). The pH by CESM2-WACCM-FV2 was under-simulated for the entire year when compared to the results of Chakraborty *et al.*[21]. During November–December, both pH values were similar. During the summer monsoon, the selected CMIP6 model and regional simulation results of Chakraborty *et al.*[21] were similar, but the CESM2-WACCM-FV2 model predicted a lower pH. During the winter monsoon, the difference between regional simulation and the CMIP6 model was large.

We aimed to model the drivers of pH[20,22] and explore the physical factors affecting the seasonality of pH for the North BoB region, where the main parameters were SST, DIC and SSS due to the influx of many rivers into the basin. Joshi and Warrior[23] used a coupled physical and biogeochemical model (ROMS + PISCES) to understand the influence of distinct drivers and mechanisms on the sea-surface pCO_2 and air–sea CO_2 flux in BoB. The most striking observation to emerge from this study was how the various sea surface parameters (SST, SSS, total alkalinity, DIC) affected the pCO_2 of BoB in controlled numerical runs. With regard to pH, similar control runs were done. One of the most important findings is related to their[23] numerical sensitivity study, which showed the correlation between the total pH increase and contribution due to SSS to be 0.87 (Figure 6) for the BoB. Figure 6 is shows that like SST, SSS and hence FWS are the primary factors affecting pH in the North BoB.

Focusing on the observational evidence, in the premonsoon season, the coastal North BoB gets seasonally stratified, and the influence of SST is to decrease the pH and increase the acidity (Figure 7). It must be noted here that the

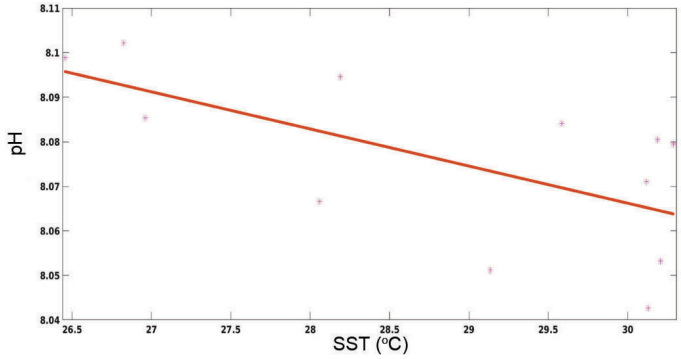

Figure 8. Correlation between pH and sea surface temperature (SST) for CESM-WACCM-FV; $R^2 = -0.63$.

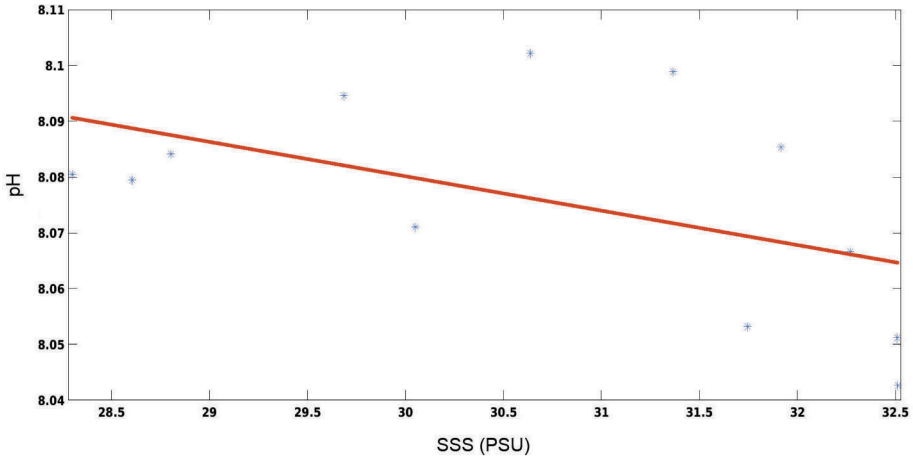

Figure 9. Correlation between pH and SSS for CESM-WACCM-FV; $R^2 = -0.5$.

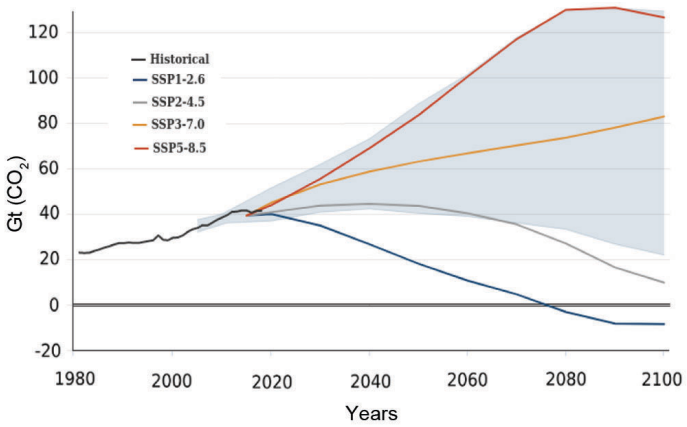

Figure 10. CMIP6 socio-economic CO_2 emission scenarios (source: https://carbonbrief.org/cmip6-the-next-generation-of-climate-models-explained).

pH contours have been taken from the second-best model (CESM-WACCM-FV) since the best model for SSS prediction (CIESM) does not have pH data. Figure 7 shows that pH strongly follows FWS in various seasons. The correlation between SSS and pH is interesting because of the enormous implications that the rivers have on the ecosystem of BoB.

Figures 8 and 9 show the correlation of pH with SST and SSS respectively, in the second best model (CESM2-WACCM-FV). These figures are plotted from the CMIP6 model. We show here a temporal correlation between the variables plotted for a point close to the coast in the northeast BoB. In Figures 8 and 9, there is a clear trend of decreasing pH with an increase in SST and SSS[24].

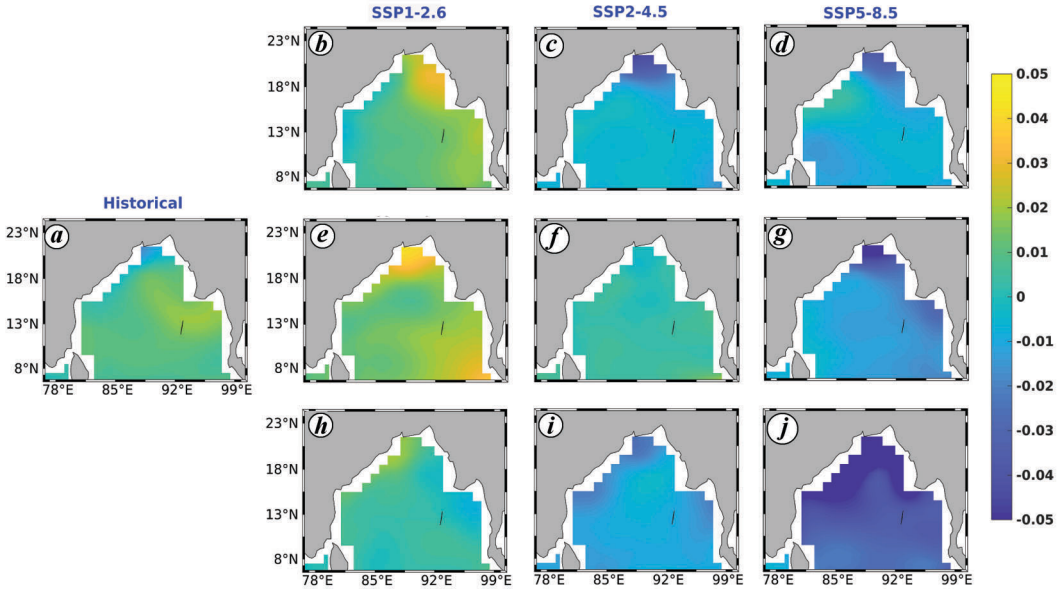

Figure 11. CIESM model trend based on the (***a***) historical period, viz. 1990–2014, (***b***) near future (2025–50) trend, (***e***) mid-century (2051–75) trend, (***h***) end–century (2076–2100) trend for SSP1-2.6 socio-economic scenarios. (***c***) near-future (2025–50) trend and (***f***) mid-century (2051–75) trend and (***i***) end-century (2076–2100) trend for the SSP2-4.5 socio-economic scenarios, (***d***) near future (2025–50) trend, (***g***) mid-century (2051–75) trend and (***j***) end-century (2076–2100) trend for the SSP5-8.5 socio-economic scenarios.

Future projections

The spatial and temporal analysis of the CMIP6 family historical simulations helps us narrow down our focus to the best model (CIESM). Figure 10 exhibits the futuristic CO_2 emission socio-economic pathways of the CMIP6 models considered for this study. SSP1-2.6 shows a gradual decline in CO_2 emission, and this is expected to increase the global mean temperature by 1.7°C by the year 2100 (ref. 22). The worst-case scenario (SSP5-8.5) indicates that by the end of this century, the temperature will increase by 4.9°C. Here we consider the CIESM model to explore the future projections of SSS in the BoB region.

It would be beneficial to project SSS for this region of BoB since it strongly affects the ecosystem here. In this study, SSS in the BoB region is projected for the period 2015–25. The historical data for 1990–2014 have been considered a reference for performing trend analysis. Figure 10 shows the trend for the three available scenarios for a period of 100 years. These trends help us understand the expected changes in the given socio-economic scenarios in the immediate future.

Figure 11 *a* shows spatially heterogenic historical trends over the BoB. It is apparent that an increasing trend in SSS is observed all over the region except in the northern bay. Evaporation, wind direction, seawater circulation, and changes in freshwater influx cause variations in SSS. Sridevi and Sarma[19] observed a decreasing trend in SSS in the North and vice versa in the South. During the northeast monsoon (NEM) season, the decrease in SSS in the northern BoB was reported to be above 0.03/year, whereas there was a significant increase in SSS in the southern BoB (0.03/year). During the deglaciation period, the melting of the ice sheet resulted in the ingestion of freshwater into the oceans. BoB is a hub for some of the world's largest rivers, which bring in large volumes of freshwater. This freshwater discharge impacts the seasonality of SSS. Jana *et al.*[8] studied the effect of rivers in the BoB using model simulations. They showed an improvement of about 50–70% in near-surface salinity, freshwater plume, stratification by the addition of rivers.

The BoB basin receives a large amount of freshwater from several rivers with a well-defined seasonal cycle. This varying seasonal freshwater contributes to variation in SST and SSS (especially in the North). During the SWM season, freshwater discharge from the rivers reaches its peak, resulting in freshening of the bay. We observed a positive percentage change during SWM in all three scenarios (Figure 11 *d–f*) in the near future. These prevailed in the central and northeastern regions too, with higher magnitudes in the north. The increase in SSS during the historical period intensified in the northern and northeastern regions.

The BoB region receives less freshwater during NEM than SWM monsoon. During NEM, freshwater from the northeast advects out of the BoB, along the coast, by the action of the EICC current system[20]. We observed a similar positive percentage change in all three scenarios in the near future. Figure 11 *g–i* shows the spatial percentage change for SSP1-2.6, SSP2-4.5 and SSP5-8.5 scenarios. We observed a greater percentage change during NEM in the near future. The northwestern Bay showed a pool (15°N–23°N) of

high negative percentage changes, formed possibly due to freshwater run-off from the north and northwestern rivers. While the rest of the bay showed a high positive percentage change (≈1.5%) for all three scenarios.

Summary and conclusion

Research has shown that accurate SSS predictions and variations increase the predictability of ocean climate for the BoB region using CMIP6 models. The historical simulation of these models was compared with the Aquarius and Argo data. This helped in analysing the capability of the models to simulate SSS in the region. We selected the top five models based on skill scores (Taylor skill score, *M*-score and Willmott skill score) using both the reference data. Our findings reveal that the CIESM model is the best for both reference data (Aquarius and Argo) and was used for further analysis.

CIESM and CASM2-WACCM-FV2 models were employed to study FWS and pH in the Bay. As expected, SSS was influenced by the movement of freshwater from the rivers as a low-salinity plume. Also, pH in BoB was interconnected with SSS due to freshwater flux. Together, these results provide important insights into the dynamic mechanisms of SSS, pH and the biological life therein.

A CMIP6 model for studying salinity has been presented and shown to provide good predictions for simulating FWS in BoB. Such an approach was found to give good-quality results in the prediction of derived parameters like pCO_2, pH and the distribution of freshwater plumes. Further analysis showed that not obtaining the flow of these thermohaline plumes (because of using other CMIP6 models) might sometimes lead to erroneous predictions of the biological life and ecosystem dynamics there.

1. Arias, P. A. *et al.*, Technical summary. *Climate Change*, 2021, **51**, 221–227.
2. Vinayachandran, P. *et al.*, A summer monsoon pump to keep the Bay of Bengal salty. *Geophys. Res. Lett*., 2013, **40**(9), 1777–1782.
3. Shetye, S. *et al.*, Hydrography and circulation in the western Bay of Bengal during the northeast monsoon. *J. Geophys. Res.: Oceans*, 1996, **101**(C6), 14011–14025.
4. Vinayachandran, P., Murty, V. and Ramesh Babu, V., Observations of barrier layer formation in the Bay of Bengal during summer monsoon. *J. Geophys. Res.: Oceans*, 2002, **107**(C12), SRF–19.
5. Thadathil, P. *et al.*, Surface layer temperature inversion in the Bay of Bengal: main characteristics and related mechanisms. *J. Geophys. Res.: Oceans*, 2016, **121**(8), 5682–5696.
6. Valsala, V., Singh, S. and Balasubramanian, S., A modeling study of interannual variability of Bay of Bengal mixing and barrier layer formation. *J. Geophys. Res.: Oceans*, 2018, **123**(6), 3962–3981.
7. Prasanna Kumar, S. *et al.*, Why is the Bay of Bengal less productive during summer monsoon compared to the Arabian Sea? *Geophys. Res. Lett*., 2002, **29**(24), 88–101.
8. Jana, S., Gangopadhyay, A. and Chakraborty, A., Impact of seasonal river input on the Bay of Bengal simulation. *Continent. Shelf Res.*, 2015, **104**, 45–62.
9. Behara, A. and Vinayachandran, P., An OGCM study of the impact of rain and river water forcing on the Bay of Bengal. *J. Geophys. Res.: Oceans*, 2016, **121**(4), 2425–2446.
10. UNESCO, Discharge of Selected Rivers of the World: A Contribution to the International Hydrological Decade, 1969.
11. Feely, R. A., Doney, S. C. and Cooley, S. R., Ocean acidification: present conditions and future changes in a high CO_2. *Oceanography*, 2009, **22**(4), 36–47.
12. Kumar, V., Joshi, A. and Warrior, H., Assessment of the CMIP6 models to study interseasonal SST variabilities in the BoB. *ISH J. Hydraul. Eng*., 2022, **43**, 1–9.
13. Sumangala, D. and Warrior, H., Coastal modelling incorporating artificial neural networks for improved velocity prediction. *ISH J. Hydraul. Eng*., 2022, **28**(*Suppl. 1*), 261–271.
14. Warrior, H. and Carder, K., An optical model for heat and salt budget estimation for shallow seas. *J. Geophys. Res.: Oceans*, 2007, **112**(C12).
15. Lin, X., Qiu, Y., Cha, J. and Guo, X., Assessment of Aquarius sea surface salinity with Argo in the Bay of Bengal. *Int. J. Remote Sensing*, 2019, **40**(22), 8547–8565.
16. Momin, I. M., Mitra, A. K., Prakash, S., Mahapatra, D., Gera, A. and Rajagopal, E., Variability of sea surface salinity in the tropical Indian Ocean as inferred from Aquarius and *in situ* datasets. *Int. J. Remote Sensing,* 2015, **36**(7), 1907–1920.
17. Du, Y., Zhang, Y. and Shi, J., Relationship between sea surface salinity and ocean circulation and climate change. *Sci. China Earth Sci.*, 2019, **62**(5), 771–782.
18. Sreeush, M. G., Rajendran, S., Valsala, V., Pentakota, S., Prasad, K. and Murtugudde, R., Variability, trend and controlling factors of Ocean acidification over western Arabian Sea upwelling region. *Mar. Chem*., 2019, **209**, 14–24.
19. Sridevi, B. and Sarma, V., Role of river discharge and warming on ocean acidification and pCO_2 levels in the Bay of Bengal. *Tellus B*, 2021, **73**(1), 1–20.
20. Madkaiker, K., Valsala, V., Sreeush, M. G., Mallissery, A., Chakraborty, K. and Deshpande, A., Understanding the seasonality, trends and controlling factors of Indian Ocean acidification over distinctive bio-provinces. *J. Geophys. Res*., 2023, 128; https://doi.org/10.1029/2022JG006926.
21. Chakraborty, K., Valsala, V., Bhattacharya, T. and Ghosh, J., Seasonal cycle of surface ocean pCO_2 and pH in the northern Indian Ocean and their controlling factors. *Prog. Oceanogr.,* 2021, **198**, 102683.
22. Gidden, M. J. *et al.*, Global emissions pathways under different socioeconomic scenarios for use in CMIP6: a dataset of harmonized emissions trajectories through the end of the century. *Geosci. Model Dev*., 2019, **12**(4), 1443–1475.
23. Joshi, A. and Warrior, H., Comprehending the role of different mechanisms and drivers affecting the sea-surface pCO_2 and the air–sea CO_2 fluxes in the Bay of Bengal: a modeling study. *Mar. Chem.*, 2022, **83**, 245–251.
24. Sarma, V., Krishna, M., Paul, Y. and Murty, V., Observed changes in ocean acidity and carbon dioxide exchange in the coastal Bay of Bengal – a link to air pollution. *Tellus B*, 2015, **67**(1), 24638.

Received 27 May 2022; re-revised accepted 23 February 2023

doi: 10.18520/cs/v124/i11/1290-1299